IOPscience iopscience.iop.org

Home Search Collections Journals About Contact us My IOPscience

Magnetophotoluminescence studies of $In_xGa_{1-x}As_{1-y}N_y$: a measurement of the electron effective mass, exciton size, and degree of carrier localization

This article has been downloaded from IOPscience. Please scroll down to see the full text article.

2004 J. Phys.: Condens. Matter 16 S3187

(http://iopscience.iop.org/0953-8984/16/31/014)

View the table of contents for this issue, or go to the journal homepage for more

Download details:
IP Address: 129.252.86.83
The article was downloaded on 27/05/2010 at 16:22

Please note that terms and conditions apply.

INSTITUTE OF PHYSICS PUBLISHING JOURNAL OF PHYSICS: CONDENSED MATTER

J. Phys.: Condens. Matter **16** (2004) S3187–S3200 PII: S0953-8984(04)74537-3

Magnetophotoluminescence studies of $In_xGa_{1-x}As_{1-y}N_y$: a measurement of the electron effective mass, exciton size, and degree of carrier localization

A Polimeni, F Masia, G Baldassarri Höger von Högersthal and M Capizzi

INFM—Dipartimento di Fisica, Università di Roma 'La Sapienza', Piazzale A Moro 2, 00185 Roma, Italy

Received 7 January 2004
Published 23 July 2004
Online at stacks.iop.org/JPhysCM/16/S3187
doi:10.1088/0953-8984/16/31/014

Abstract

Photoluminescence (PL) under a magnetic field ($B = 0$–12 T) has been employed to determine the electron effective mass, m_e^*, exciton radius, r_{exc}, and degree of localization of carriers in $In_xGa_{1-x}As_{1-y}N_y$/GaAs heterostructures. This study concerns nitrogen concentration values spanning from a very dilute ($y < 0.1\%$) to a full alloy ($y = 5\%$) limit and indium concentrations x from 0% to ∼30%. For indium-free samples, we find that m_e^* and r_{exc} undergo a sudden increase and squeezing, respectively, for $y \sim 0.1\%$. For indium-containing samples ($x \sim 30\%$), m_e^* and r_{exc} show a sudden variation similar to that for $x = 0$ but shifted to much higher N concentration ($y \sim 1\%$). In addition, in the N alloy limit the temperature dependence of the B-induced shift of the PL peak position reveals that radiative recombination at low temperature is not excitonic.

1. Introduction

Recently, nitrogen incorporation in $In_xGa_{1-x}As$-based materials has attracted much interest owing to the strong modifications exerted by N on the band structure of the host lattice [1]. These include a giant band gap reduction [1] and a decrease in the rate at which the band gap depends on hydrostatic pressure [2, 3] and temperature [4, 5]. Moreover, a strong dependence of the electron effective mass, m_e, on the nitrogen concentration has been found by a variety of experimental techniques [6–14]. The introduction of N in the host lattice is also a source of a high degree of disorder, which manifests itself in the optical properties of the material. This leads to a sizable inhomogeneous broadening of the radiative transitions [4], to a large Stokes shift between absorption and emission [15], and to the presence of localized states, which at low temperature often dominate the emission spectra [4, 5]. Moreover, from a more fundamental standpoint the highly disordered potential arising from the large fluctuations induced by N

 © 2004 IOP Publishing Ltd Printed in the UK

might undermine a representation of the crystal electronic states in terms of coherent Bloch states with a well-defined $\boldsymbol{k}$ vector [16]. In turn, this could invalidate an effective mass scheme for describing the electronic properties of $In_xGa_{1-x}As_{1-y}N_y$.

In this paper, we report on a comprehensive study of the effects of a magnetic field ($B = 0$–12 T) on the photoluminescence (PL) properties of $In_xGa_{1-x}As_{1-y}N_y$/GaAs heterostructures. Such study is aimed at the measurement of the properties of the bottom of the conduction band (both curvature and localization degree) of N-containing samples. We describe first the evolution of the electron effective mass and exciton radius, r_{exc}, in $GaAs_{1-y}N_y$ epilayers with N concentration varying from $y < 0.01\%$ to $y = 0.5\%$. In particular, by exploiting the capability of post-growth hydrogen irradiation to finely tune the electronic properties of $GaAs_{1-y}N_y$ [17–21], we assess that a major change in m_e^* and in r_{exc} takes place within a very narrow concentration interval centred at $y = 0.1\%$. We consider then the magneto-PL properties of $In_xGa_{1-x}As_{1-y}N_y$/GaAs quantum wells, QWs, having $x \sim 30\%$ and $y = (0.7–5.2)\%$. For these samples, the electron effective mass (exciton radius) increases (decreases) with y up to a N concentration equal to 1%, namely, an order of magnitude higher than that found in In-free samples. We finally show how magneto-PL provides a clue to the localized versus delocalized nature of the recombining carriers at low temperature in $In_xGa_{1-x}As_{1-y}N_y$ samples in the alloy limit. Indeed, the shift of the PL bands induced by B decreases sizably and changes its dependence on B from linear to quadratic on going from low to high T. These findings indicate that the PL emission at low temperature is determined by the recombination of loosely bound electron–hole pairs in which one carrier is localized by N-induced potential fluctuations and the other carrier is delocalized.

2. Experimental details

The samples considered in this paper were grown on (001)-oriented GaAs by different techniques. One set of samples consists of four 0.5 μm thick $GaAs_{1-y}N_y$ epilayers ($y =$ 0.043%, 0.1%, 0.21%, 0.5%) grown by metal–organic vapour phase epitaxy [22, 23]. The sample with $y = 0.1\%$ has been hydrogenated at 300 °C by a low energy ion gun (beam energy ∼100 eV). Another set of samples were grown by solid source molecular beam epitaxy and they consist of 300 nm thick $GaAs_{1-y}N_y$ epilayers having $y < 0.01\%$ and $In_xGa_{1-x}As_{1-y}N_y$/GaAs single quantum wells having $x = (25–42)\%$, $y = (0.7–5.2)\%$, and QW thickness $L = 6.0–8.2$ nm. The sample composition and thickness were determined by x-ray diffraction measurements. PL measurements have been carried out in a liquid He optical cryostat for T ranging from 10 to 200 K. The magnetic field was applied parallel to the growth axis of the samples. PL was excited by the 515 nm line of an Ar^+ laser or the 532 nm line of a vanadate–YAG laser, dispersed by a double 3/4 m monochromator, and detected by a N-cooled Ge detector or by a N-cooled InGaAs linear array.

3. Electron effective mass and exciton size in $GaAs_{1-y}N_y$

We consider first the magneto-PL properties of $GaAs_{1-y}N_y$ epilayers whose PL spectra at low temperature and zero magnetic field are shown in figure 1. At the very early stage of N incorporation in GaAs (N concentration less than 0.01%, bottommost curve in figure 1), the PL spectrum is characterized by a number of sharp lines (linewidth ∼0.5 meV) between 1.40 and 1.48 eV. These lines are attributed to carrier recombination from electronic levels due to N pairs and/or clusters [22–28] and are superimposed on a broad band also related to N incorporation. The luminescence intensity of these transitions varies from line to line and

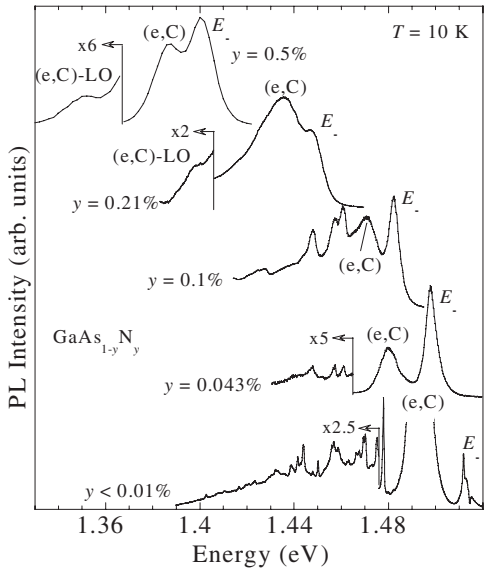

Figure 1. Low temperature (10 K) PL spectra of $GaAs_{1-y}N_y$ epilayers with different y's. E_- and (e, C) indicate the free-exciton and free-electron to neutral carbon acceptor recombinations, respectively. (e, C)-LO indicates the longitudinal optical phonon replica of the (e, C) transition.

increases with y (not shown here). An exact assignment of each line to a given N complex is made rather difficult by the strong dependence of the material optical properties on the growth conditions, as extensively reported in the literature [24, 26–28]. Free-electron to neutral carbon acceptor, (e, C), and free-exciton, E_-, recombinations of GaAs are observed at 1.493 and 1.515 eV, respectively. As the nitrogen concentration is increased further ($y = 0.043$ and 0.1%), the energy of the excitonic recombination from the material's band gap, E_-, as well as the (e, C) recombination band start red-shifting very rapidly, coexisting with and taking in the levels associated with the N complexes. The energy of these levels does not change with N concentration [22, 26, 27]. These features highlight the strongly localized character of the N isoelectronic traps, in contrast to that of shallow impurities whose wavefunctions overlap at smaller concentrations (10^{16}–10^{18} cm^{-3}). Eventually at higher N concentrations (alloy limit, $y > 0.1\%$) the $GaAs_{1-y}N_y$ band gap keeps red-shifting [29] along with the C related states.

The dramatic variation of the GaAs host band gap upon N incorporation is accompanied by other major effects on the electronic and optical properties of the lattice. Of all of these effects the variation in the electron effective mass is one of the most controversial. A large scatter in the data reported so far is found, indeed [6–14]. We describe now a method for deriving the electron effective mass and exciton wavefunction extent in $GaAs_{1-y}N_y$ by using the effect of a magnetic field on the electronic states associated with the material's conduction band. In particular, we show how a controlled introduction of H in the lattice allows monitoring the evolution of m_e^* and r_{exc} upon variation in the effective concentration of N present in the samples.

Figure 2(a) shows the PL spectra of a $GaAs_{1-y}N_y$ epilayer with $y = 0.1\%$ recorded under different magnetic field values. Figure 2(b) shows the magnetic field dependence of the energy for different recombination curves, whose attribution has been discussed previously. PL spectra have been taken at about 30 K to reduce the contribution from donor–acceptor pair recombination. On applying a magnetic field, all PL lines below 1.462 eV (open circles) remain

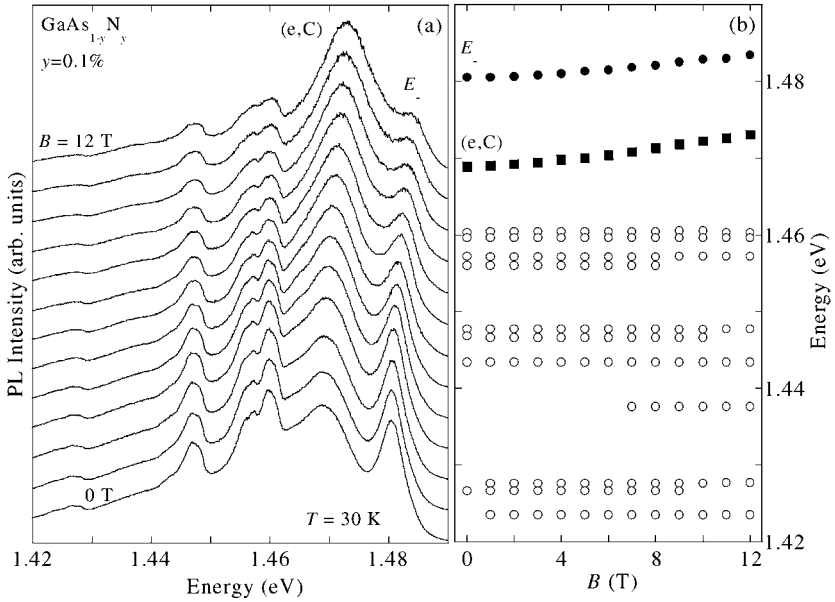

Figure 2. (a) PL spectra at $T = 30$ K of a $GaAs_{0.999}N_{0.001}$ epilayer recorded under different magnetic fields, B. (e, C) indicates the free-electron to neutral carbon recombination and E_- indicates the free-exciton recombination. Other recombination curves below 1.462 eV are related to N complex states. (b) The B dependence of the peak energy of the different recombination bands observed in part (a). Note that only the (e, C) and E_- transitions display a sizable shift with B.

pinned in energy, consistently with the highly localized nature expected for N cluster states. In contrast, the E_- (full circles) and (e, C) (full squares) bands blue-shift with increasing B. The behaviour of these bands with B is consistent with their extended nature. Similar findings have been observed in all samples shown in figure 1.

As an example, the PL spectra of samples with $y = 0.043\%$ (dilute limit) and 0.21% (alloy limit) are shown in panels (a) and (b) of figure 3, respectively, for different B values. The B-induced diamagnetic shift, $\Delta E_d = E(B) - E(0)$, of the E_- and (e, C) recombination lines is shown as a function of B in panels (c) and (d) of figure 3 for the two samples. The E_- band shifts with B at a lower rate than the (e, C) band, owing to the larger Coulomb attraction between the electron and hole in the former case. Values of the electron effective mass, to be discussed later, have been estimated by fitting (dashed curves; see panels (c) and (d) in figure 3) the formula for the magnetic field dependence of the bottommost Landau level of the conduction band, $\Delta E_d = \beta B = (\hbar e/2m_e^*)B$, to the shift of the (e, C) transition in the B-linear region of ΔE_d [30]. At zero magnetic field, ΔE_d extrapolates to a negative value, of the order of $k_B T/2$, as found in other magneto-PL measurements of the B-induced shift of free-electron to neutral acceptor recombinations [31–33]. This behaviour is usually attributed to the change in the density of states of the system from three- to one-dimensional due to the applied magnetic field. The continuous curves in panels (c) and (d) of figure 3 are fits of $\Delta E_d = \alpha B^2 = e^2\langle r_{eh}^2\rangle/(8\mu)B^2$ to the E_- diamagnetic shift in the low field regime (small perturbation limit). r_{eh} and μ are the electron–hole distance and the reduced effective mass of excitons, respectively. At very low N concentration, α rapidly decreases by a factor of $\sim$2 with respect to the value it has in GaAs and tends to saturate for $y > 0.1\%$. This behaviour matches well that found for m_e^*. By using the m_e^* values determined from the slope of the (e, C)

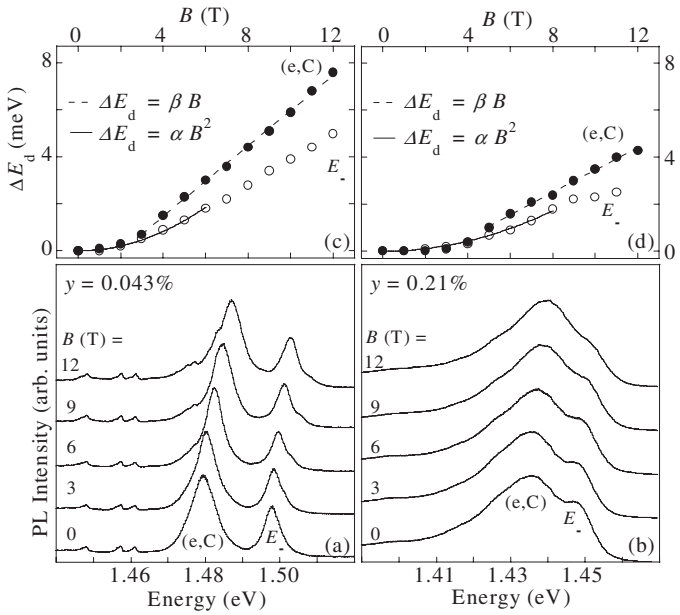

Figure 3. Panels (a) and (b) show the PL spectra of $GaAs_{1-y}N_y$ samples with $y = 0.043\%$ and 0.21%, respectively, taken at different magnetic fields ($T = 30$ K). (e, C) indicates the free-electron to neutral carbon recombination and E_- indicates the free-exciton recombination. Panels (c) and (d) show the B-induced shift value, ΔE_d, of the (e, C) (full symbols) and of the E_- (open symbols) peak energy, as a function of the magnetic field, for the corresponding samples shown in the lower panels. The dashed (continuous) curves are fits of a linear (quadratic) B dependence to the ΔE_d values of the (e, C) (E_-) peak. Note that the data on the E_- transition in the $y = 0.21\%$ sample have been derived from magneto-PL spectra recorded at higher laser power to better determine the transition peak energy (not shown here).

transition and the diamagnetic shift formula $\Delta E_d = \alpha B^2$, we get an estimate of $r_{exc} = \sqrt{\langle r_{eh}^2 \rangle}$ for each sample, to be discussed later[1].

In order to follow closely the variation of m_e^* and r_{exc} with the N effective concentration, we performed a study similar to that described above on a sample irradiated at different H doses. As already reported by us, H tunes in a controllable and reversible way the electronic properties of $In_xGa_{1-x}As_{1-y}N_y$ and $GaP_{1-y}N_y$ [17–21, 34]. This is illustrated in figure 4 for a $GaAs_{1-y}N_y$ epilayer ($y = 0.1\%$). H irradiation leads first to a passivation of the N cluster states (see the second curve from the bottom) and then to an apparent reopening of the $GaAs_{1-y}N_y$ band gap toward that of the GaAs reference (topmost continuous curve). As a matter of fact, both the (e, C) and the E_- recombination bands converge to those of the GaAs reference with increasing H dose, as shown by continuous curves in figure 4. On applying a magnetic field (see the dashed curves in figure 4), the E_- and (e, C) bands blue-shift with increasing B. Notice that the energy separation between these two transitions increases on going from the H-free to the H-treated samples, due to a corresponding decrease in the tensile strain with decreasing effective N concentration [35]. In fact, for decreasing N concentration

[1] As for the hole effective mass, the increasing tensile strain with increasing y modifies the top of the valence band character from prevalently heavy to light. We get an estimate of the hole mass (m_h^*) variation from the measured change in the acceptor binding energy roughly estimated by the energy difference between the free exciton and the (e, C) recombination by setting $m_h^* = 0.45\, m_0$ as the starting point for $y = 0\%$.

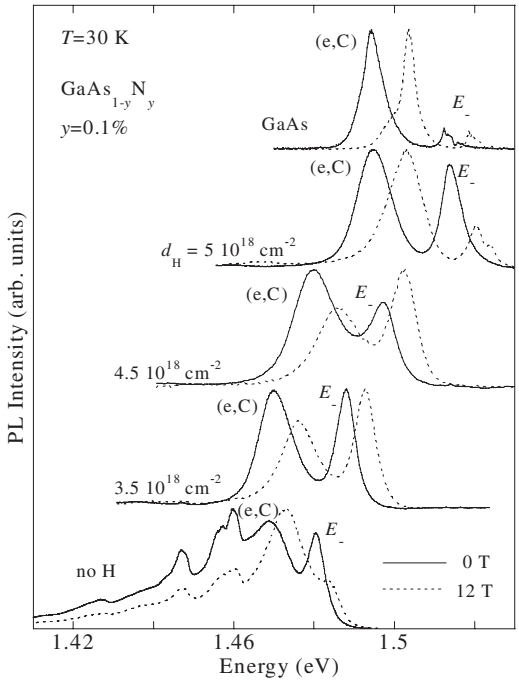

Figure 4. PL spectra at $T = 30$ K of a $GaAs_{0.999}N_{0.001}$ alloy treated with different hydrogen doses d_H. The bottommost and topmost spectra refer to an untreated $GaAs_{1-x}N_x$ and a reference GaAs sample, respectively. Continuous and dashed curves indicate PL spectra taken under zero and 12 T magnetic field, respectively. (e, C) indicates the free-electron to neutral carbon recombination and E_- indicates the free-exciton recombination. Different laser power densities have been employed for the different samples in order to highlight the presence of both (e, C) and E_- bands.

the top of the valence band acquires a more pronounced heavy-hole character and, in turn, the binding energy of the acceptor impurity increases.

The energy shifts, ΔE_d, of the (e, C) and E_- recombination lines are shown as a function of B in figures 5(a) and (b), respectively, for $GaAs_{1-y}N_y$ (both untreated and hydrogenated, full symbols) and for the GaAs reference (open symbols). The same analysis performed for the untreated samples (see figure 3) has been applied to the hydrogenated samples. We point out that the slope of the line fitting the (e, C) transitions increases with increasing H dose until the value of the GaAs reference is obtained, as shown in figure 5(a). A similar recovery of the pristine GaAs properties can be observed in the dependence of the exciton diamagnetic shift displayed in figure 5(b). In particular, the inset of figure 5(b) shows a fit of $\Delta E_d = [e^2\langle r_{eh}^2\rangle/(8\mu)]B^2$ to the E_- data in the quadratic, low field region. Consistently with the H-induced m_e^* decrease, the exciton size increases upon hydrogenation.

Finally, figures 6(a) and (b) show, respectively, the electron effective mass and exciton size as a function of the peak energy of the band gap exciton. We point out that sound values of both m_e (=0.065 m_0, where m_0 is the vacuum electron mass) and r_{exc} (=15.3 nm, which corresponds to an exciton Bohr radius $a_0^{exc} = r_{exc}/\sqrt{3} = 8.8$ nm) are obtained for the GaAs reference. Full dots refer to the $GaAs_{1-y}N_y$ alloy with $y = 0.1\%$ for both the untreated sample (grey symbol) and the hydrogenated samples (black symbols). The grey full triangles are the m_e^* and r_{exc} values measured for non-hydrogenated samples with different N concentrations ($y = 0$, $y < 0.01\%$, $y = 0.043\%$, 0.21%, and 0.5%). Both m_e^* and r_{exc} vary bi-uniquely

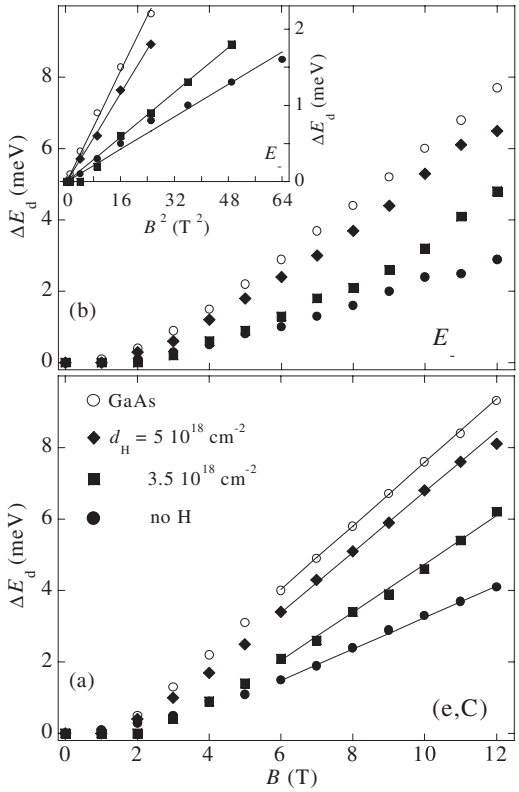

Figure 5. (a) The energy shift with magnetic field of the free-electron to neutral carbon recombination (e, C) for some of the samples shown in figure 4. The continuous curves are a fit to the data by $\Delta E_d = (\hbar e/2m_e^*)B$. The electron effective mass m_e^* is derived directly from the line slope. (b) The energy shift with magnetic field of the free-exciton recombination E_-. The samples considered are the same as in part (a). The inset highlights the low field part of the graph and displays the E_- energy dependence on B^2. The straight lines are a fit of $\Delta E_d = [e^2\langle r_{eh}^2\rangle/(8\mu)]B^2$ to the data, where $\langle r_{eh}^2\rangle$ is a fit parameter.

with the sample band gap energy, that is, they depend on the *effective* N concentration in the crystal regardless of how this concentration has been achieved (either by N incorporation in GaAs or by H irradiation of $GaAs_{1-x}N_x$). Most importantly, these findings allow monitoring the evolution of the electronic properties of $GaAs_{1-y}N_y$ in a virtually continuous manner. In particular, the electron effective mass increases very rapidly from the GaAs value (=0.065 m_0 as derived here) to ∼0.13 m_0 for $E_- \sim 1.48$ eV and reaches slowly a value of ∼0.14 m_0 for $E_- \sim 1.4$ eV. Accordingly, the exciton size undergoes a shrinking with increasing N effective concentration and varies from $r_{exc} = 15.3$ nm in GaAs to 9.5 nm in $GaAs_{0.995}N_{0.005}$. The fast decrease in r_{exc} provides further evidence that N-induced localization effects start at very low values of y.

4. Electron effective mass and exciton size in $In_xGa_{1-x}As_{1-y}N_y$

We now describe magneto-PL measurements performed on $In_xGa_{1-x}As_{1-y}N_y$/GaAs QWs having $0.007 \leqslant y \leqslant 0.052$.

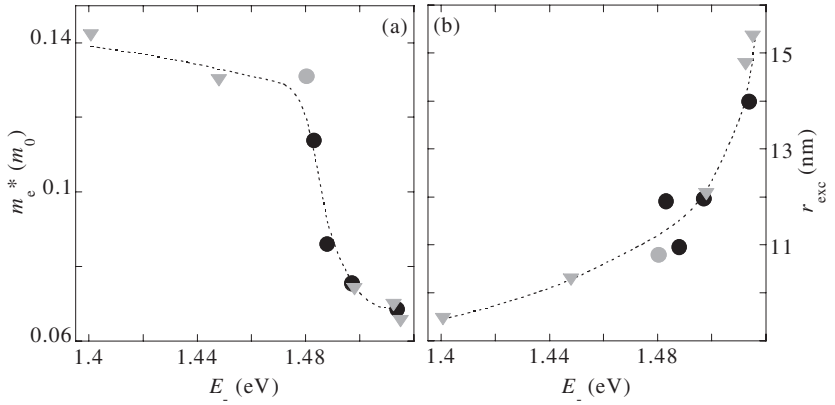

Figure 6. (a) The electron effective mass dependence on the free-exciton peak energy at 10 K. Full dots refer to an untreated (grey) and hydrogenated (black) $GaAs_{0.999}N_{0.001}$ samples; grey triangles refer to $GaAs_{1-y}N_y$ epilayers with different y values. (b) The exciton size dependence on the free-exciton peak energy at 10 K. Symbols have the same meaning as in part (a). Dashed curves are guides to the eye.

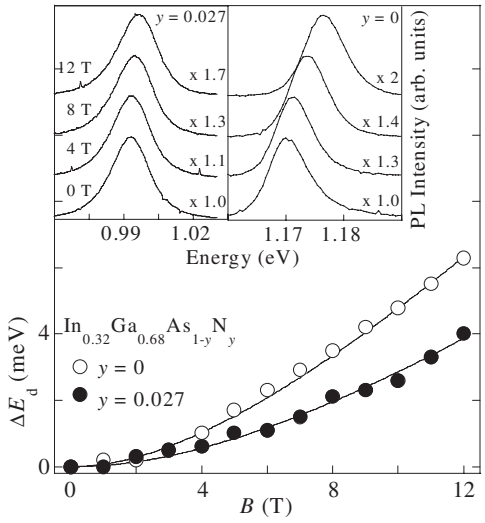

Figure 7. The diamagnetic shift, ΔE_d, measured at $T = 100$ K in an $In_{0.32}Ga_{0.68}As_{0.973}N_{0.027}$ QW (full circles) and in an $In_{0.32}Ga_{0.68}As$ reference QW (open circles) versus magnetic field B. The continuous curves are fits of equation (1) to the data (the values of the only fitting parameter $\mu_\parallel$ are 0.039 m_0 and 0.049 m_0 for $y = 0$ and 0.027, respectively). The inset shows the PL spectra of these two samples at representative magnetic field values. Multiplication factors are given. Laser power density $P = 20$ W cm^{-2}.

The inset of figure 7 shows the PL spectra recorded on an $In_{0.32}Ga_{0.68}As_{0.973}N_{0.027}$ QW and an $In_{0.32}Ga_{0.68}As$ reference QW for representative B values. The PL spectra have been taken at relatively high temperature ($T = 100$ K) in order to eliminate the contribution of localized states as will be discussed in the next section. In both samples the PL intensity increases with increasing B due to a squeezing of the exciton wavefunction in the plane perpendicular to the field direction. The diamagnetic shift of the PL peak energy E_p is shown in figure 7 for the two

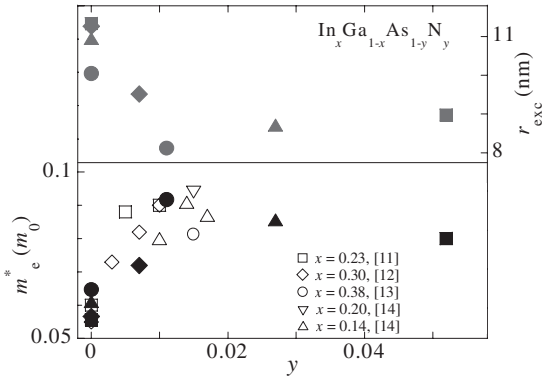

Figure 8. Lower panel: the N concentration dependence of the electron effective mass m_e^* for the samples studied in this work (full symbols: $x = 0.25$ (●), $x = 0.32$ (▲), $x = 0.34$ (♦), and $x = 0.38$ (■)) and taken from the literature (open symbols). PL data have been taken at $T = 180$ K ($y = 0.007$ and 0.011), and at $T = 150$ K ($y = 0.027$ and 0.052). Upper panel: the N concentration dependence of the exciton radius, r_{exc}, for the samples studied in this work (full symbols: $x = 0.25$ (●), $x = 0.32$ (▲), $x = 0.34$ (♦), and $x = 0.38$ (■)).

samples as a function of B. The presence of a few per cent of N atoms leads to ΔE_d values quite a bit smaller than those measured in the reference QW.

In our samples, the magnetic energy $\hbar\omega_c$ ($=\hbar eB/\mu_\parallel$, $\mu_\parallel$ being the exciton reduced mass in the plane perpendicular to B) for $In_{0.3}Ga_{0.7}As$ is about 18 meV at 6 T, that is, of the order of the expected exciton binding energy (∼10 meV). Therefore, the linear B (Landau levels) or the quadratic B^2 (perturbation theory) usual approximations do not hold over the whole (0–12) T field interval investigated here. Then, we analyse the diamagnetic shift data by using a numerical method proposed by MacDonald and Ritchie [36][2], for two-dimensional Coulombic systems at arbitrary magnetic fields. On the basis of this model the diamagnetic shift can be written in terms of a two-point Padé approximant

$$\Delta E_d(B; z) = \sum_{i=0}^{7} p_i z^i \Bigg/ \sum_{k=0}^{5} q_k z^k, \tag{1}$$

where p_i and q_k are numerical coefficients whose values can be found in [36], $z = \sqrt{(\varepsilon^2\hbar^3 B)/(\mu_\parallel^2 e^3 c)}$, and ε is the material dielectric constant. A very good agreement is found between the experimental data and the theoretical fits (see continuous curves obtained using $\mu_\parallel$ as the only fitting parameter) for both samples shown in figure 7—as well as for all the other $In_xGa_{1-x}As_{1-y}N_y$ samples investigated here.

We now estimate from our $\mu_\parallel$ data the electron effective mass and compare it with the experimental results reported in the literature for $In_xGa_{1-x}As_{1-y}N_y$ with high x (>10%) [11–14]. To this end we set the in-plane heavy-hole effective mass equal to 0.12 m_0, as reported in [37] for samples similar to ours. Then, we get the m_e^* values shown as a function of y by full symbols in figure 8. Data reported by other authors are shown in the same figure by open symbols. For $y \leqslant 0.01$, m_e^* increases rapidly with y, as found in [11–14] on the

[2] Note that excitons in the present samples have an enhanced two-dimensional character because of the strong confining potential provided by the high In concentration ($x \sim 0.3$) in the QWs. In addition, a reasonable criterion for establishing the applicability of the model of [36] to real QWs is that the magnetic length should be greater than or about equal to the QW thickness [55]. In our experiments the magnetic length ($=25.7/\sqrt{B}$ nm) reaches a minimum value of 7.4 nm at the highest field employed (i.e., 12 T). It is, therefore, larger than the thickness of our QWs for most of the field intensities employed.

grounds of different experimental techniques, and seems to saturate at high N concentration. The exciton radius can be estimated in the limit of a true two-dimensional system as $r_{\rm exc} = \sqrt{\langle r_{\rm eh}^2 \rangle} = \sqrt{3/8}\, a_0^{\rm exc}$ [38], where $a_0^{\rm exc}$ is the exciton Bohr radius calculated by using the exciton reduced mass $\mu_\parallel$ derived from the experimental data. The dependence of $r_{\rm exc}$ on nitrogen concentration is shown in the upper panel of figure 8.

We note that in In-containing samples the dependence of $m_{\rm e}^*$ and $r_{\rm exc}$ on nitrogen concentration displays a rapid change starting from much higher y values as compared to the $GaAs_{1-y}N_y$ case (see figure 6). This is most likely due to the greater energy distance between the CB resonant level of N and the bottom of the CB of the $In_xGa_{1-x}As$ host with respect to that of GaAs. As a consequence, this reduces the interaction between the N level and those of the host lattice conduction band for $x \neq 0$ [1].

To conclude this part, we would like to discuss briefly some implications of our effective mass measurements. In particular, one might wonder whether an envelope function approach can be used to derive an electron (and exciton) effective mass when the introduction of N atoms in the $In_xGa_{1-x}As$ lattice strongly perturbs the periodic potential with an ensuing mixing of different $\boldsymbol{k}$ vectors in the electron wavefunction. In fact, Mattila *et al* [39] have shown that the electron wavefunction at the conduction band edge has a 42% non-Γ character for $y = 0.8\%$, which results in a sizable wavefunction localization and in intrinsically short electron diffusion lengths. However, the conduction band edge state has an extended character far away from nitrogen and allows those authors to discuss the dependence of the electron effective mass of this state on nitrogen concentration [39, 40]. In addition, the values of the electron effective mass derived here are in good agreement with those reported in the literature and derived by different experimental techniques. This supports the applicability of an effective mass scheme for describing the electronic properties of the $In_xGa_{1-x}As_{1-y}N_y$ highly disordered system.

5. Single-carrier localization investigated by magnetophotoluminescence

In $In_xGa_{1-x}As_{1-y}N_y$ recombination from localized states dominates emission processes at low temperature [4, 5]. As a matter of fact, in semiconductor alloys local fluctuations in the composition lead to an exponential tail of localized states within the crystal forbidden gap [41, 42]. The preferential occupancy of these low energy states by carriers at low T is responsible for asymmetric photoluminescence spectra [4, 5, 43–49], a blue-shift of the PL peak energy as the excitation power increases [5, 46–49], a decreasing emission decay time of PL with increasing emission energy [44, 47–51], and a non-monotonic dependence of the PL maximum energy on temperature [4, 44, 48, 50]. Usually, it is assumed that radiative recombination from states induced by composition disorder is excitonic in nature. Very recently this picture has been questioned for $GaAs_{1-y}N_y$, where the fast rise time ($\sim$25 ps) of the PL signal was used to establish that radiative recombination occurs between localized electrons and delocalized holes [52]. Alternatively, the degree of localization and/or confinement of carriers in semiconductor heterostructures can be investigated through the dependence of carrier energy levels on B as measured by means of magneto-PL. The inset in figure 9 shows the PL spectra for representative B values recorded on an $In_{0.25}Ga_{0.75}As_{0.989}N_{0.011}$ QW. At $T = 30$ K the PL lineshape shows a long low energy tail characteristic of localized state recombination, which is absent at $T = 180$ K where emission is dominated by free excitons. The diamagnetic shift, $\Delta E_{\rm d}$, of the PL peak energy is shown in figure 9 as a function of B for the two measurement temperatures. The high T data have been fitted by using equation (1) (dashed curve in the figure) where the exciton reduced mass is the only fitting parameter [36]. Equation (1), which holds for two-dimensional Coulombic systems, does not fit the low T dependence of $\Delta E_{\rm d}$ on

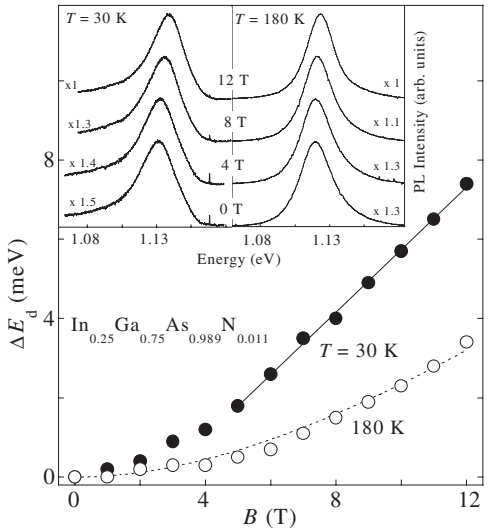

Figure 9. The diamagnetic shift, ΔE_d, of the PL peak measured in an $In_{0.25}Ga_{0.75}As_{0.989}N_{0.011}$ QW at $T = 30$ K (full dots) and $T = 180$ K (open circles) versus magnetic field, B. The dashed curve is a fit to the $T = 180$ K data for a model for two-dimensional Coulombic systems at arbitrary magnetic fields; see [36]. The continuous line is a fit to the $T = 30$ K data ($B > 4$ T) by $\Delta E_d = (e\hbar/2m_h^*)B$, where m_h^* is the in-plane hole effective mass. The inset shows the PL spectra at representative magnetic field values and different temperatures. Multiplication factors are given. Laser power density $P = 15$ mW cm^{-2} and 20 W cm^{-2} for $T = 30$ and 180 K, respectively.

B, which is linear at least for $B > 4$ T. Moreover, it should be noticed that ΔE_d is higher at low T than at high T for any value of B (a factor two for $B = 12$ T). This indicates that at low temperature the recombining electron–hole pair is more loosely bound than an *exciton*, either localized or free. Indeed, the interaction of these electron–hole pairs at low T with a magnetic field results in a perturbation stronger than the Coulomb attraction and, therefore, in a greater diamagnetic shift with respect to the exciton case. Furthermore, we point out that:

(i) ΔE_d is independent of T at high temperature where free excitons only contribute to PL,
(ii) ΔE_d measured at low T decreases when very high power densities are employed (namely, when free excitons start contributing to the PL signal),
(iii) these effects are absent in the N-free $In_xGa_{1-x}As$ QWs studied for comparison purposes.

On the basis of such observations, the PL emission at low temperature can be attributed to recombination of a localized with a delocalized carrier[3]. As for the charge of the localized carriers, one can invoke the model proposed first by Hopfield *et al* [53], who suggested that N in GaP is an isoelectronic *electron* trap. Since N in GaAs shares several common features with GaP:N, we argue that N in $In_xGa_{1-x}As$ behaves as an isoelectronic *electron* trap, too. Consequently the potential minima due to N compositional disorder capture electrons with which *free* holes can recombine, similarly to a free-hole to neutral donor recombination (this is shown schematically in the inset of figure 10). Under this hypothesis the electron is strongly localized and the shift of the PL peak with B can be ascribed entirely to the free hole, namely $\Delta E_d = (e\hbar/2m_h^*)B$ where m_h^* is the hole in-plane effective mass. The continuous line in

[3] Recombination between uncorrelated electron–hole pairs would lead to non-exponential decay curves, contrary to what is found here; see also [47].

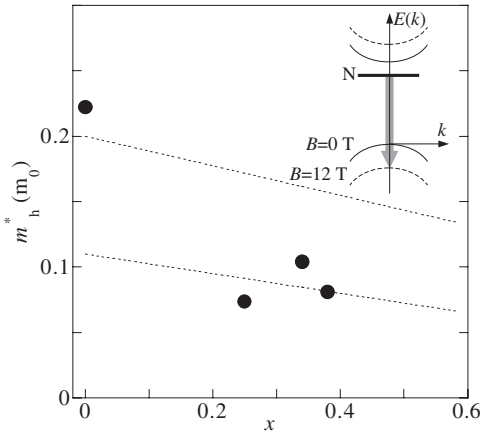

Figure 10. The dependence of the in-plane hole effective mass in $In_xGa_{1-x}As_{1-y}N_y$ as a function of the In concentration, x. The dashed lines are the values of the in-plane light (upper line) and heavy (lower line) holes, as estimated by using the Luttinger parameters; see [54]. The inset depicts the recombination at low temperature occurring in $In_xGa_{1-x}As_{1-y}N_y$ in a reciprocal space scheme at $\boldsymbol{k} \sim 0$ for $B = 0$ T (continuous parabolas) and 12 T (dashed parabolas). N indicates a localized level related to nitrogen insertion in the host lattice.

figure 9 is a fit of this formula to the $T = 30$ K data with $m^*_h = 0.074\, m_0$.[4] A similar approach has been used for deriving the electron effective mass from the B-induced shift of free-electron to neutral acceptor recombinations; see the previous section. Figure 10 shows the m^*_h values derived in $In_xGa_{1-x}As_{1-y}N_y$ QWs as a function of the In concentration. Since N incorporation affects mainly the conduction band states [1], we compare the m^*_h values derived here with those of the heavy and light hole of the N-free $In_xGa_{1-x}As$ host. In fact, due to the different type of strain, compressive in $In_xGa_{1-x}As_{1-y}N_y$ and tensile in $GaAs_{1-y}N_y$, in-plane heavy and light holes should be considered in the former and latter case. The dashed lines in figure 3 are the $In_xGa_{1-x}As$ in-plane hole masses as estimated through the Luttinger parameters [54]. The good agreement of the experimental data with the hole curves supports our hypothesis about the hole nature of the delocalized carrier.

6. Conclusions

We presented a comprehensive study of the magneto-PL properties of $In_xGa_{1-x}As_{1-y}N_y$/GaAs heterostructures. We measured the electron effective mass and exciton wavefunction extent from the very dilute to the full alloy limit of nitrogen concentration. The electron effective mass and exciton radius undergo a rapid increase and decrease, respectively, upon N incorporation in the $In_xGa_{1-x}As$ host lattice. The N concentration onset of such a rapid variation depends on the In concentration in the samples (namely, $y = 0.1\%$ for $x = 0\%$ and $y = 1\%$ for $x \sim 30\%$). The data presented provide clear-cut guidelines for theoretical models aimed at describing the puzzling electronic properties of $In_xGa_{1-x}As_{1-y}N_y$. Finally, we showed that magneto-PL sheds new light on the origin of the states from which carriers recombine at low temperature. Indeed, the counterintuitive temperature dependence of the shift of the PL peak position induced by B indicates that the PL emission at low temperature is due to the recombination of electrons localized by the N-induced potential with delocalized holes.

[4] As B approaches zero, ΔE_d deviates from a linear behaviour probably because of a residual electrostatic interaction between electrons and holes.

Acknowledgments

This work was funded by Progetto Giovani Ricercatori and COFIN 2001 (MIUR). We are grateful to Drs P J Klar and W Stolz for a most fruitful collaboration and for providing the $GaAs_{1-y}N_y$ samples and to Professor A Forchel for providing the $In_xGa_{1-x}As_{1-y}N_y$ samples.

References

[1] For a review see: Ager J and Walukiewicz W (eds) 2002 *Semicond. Sci. Technol.* **17** (special issue on III–N–V semiconductor alloys) 741
[2] Perlin P, Subramanya S, Mars D E, Kruger J, Shapiro N A, Siegle H and Weber E R 1998 *Appl. Phys. Lett.* **73** 3703
[3] Shan W, Walukiewicz W, Ager J W III, Haller E E, Geisz J F, Friedman D J, Olson J M and Kurtz S R 1999 *Phys. Rev. Lett.* **82** 1221
[4] Polimeni A, Capizzi M, Geddo M, Fischer M, Reinhardt M and Forchel A 2000 *Appl. Phys. Lett.* **77** 2870 and references therein
[5] Polimeni A, Capizzi M, Geddo M, Fischer M, Reinhardt M and Forchel A 2001 *Phys. Rev.* B **63** 195320 and references therein
[6] Hai P N, Chen W M, Buyanova I A, Xin H P and Tu C W 2000 *Appl. Phys. Lett.* **77** 1843
[7] Wu J, Shan W, Walukiewicz W, Yu K M, Ager J W III, Haller E E, Xin H P and Tu C W 2001 *Phys. Rev.* B **64** 85320
[8] Jones E D, Allerman A A, Kurtz S R, Modine N A, Bajaj K K, Tozer S W and Wie W 2000 *Phys. Rev.* B **62** 7144
[9] Zhang Y, Mascarenhas A, Xin H P and Tu C W 2000 *Phys. Rev.* B **61** 7479
[10] Gorczyca I, Skierbiszewski C, Suski T, Christensen N E and Svane A 2002 *Phys. Rev.* B **66** 081106
[11] Duboz J-Y, Gupta J A, Byloss M, Aers G C, Liu H C and Wasilewski Z R 2002 *Appl. Phys. Lett.* **81** 1836
[12] Pan Z, Li L H, Lin Y W, Sun B Q, Jiang D S and Ge W K 2001 *Appl. Phys. Lett.* **78** 2217
[13] Hetterich M, Dawson M D, Egorov A Yu, Bernklau D and Riechert H 2000 *Appl. Phys. Lett.* **76** 1030
[14] Heroux J B, Yang X and Wang W I 2002 *J. Appl. Phys.* **92** 4361
[15] Buyanova I A, Izadifard M, Chen W M, Polimeni A, Capizzi M, Xin H P and Tu C W 2003 *Appl. Phys. Lett.* **82** 3662
[16] Wang L-W, Bellaiche L, Wei S-H and Zunger A 1998 *Phys. Rev. Lett.* **80** 4725
[17] Polimeni A, Baldassarri H v H G, Bissiri M, Capizzi M, Fischer M, Reinhardt M and Forchel A 2001 *Phys. Rev.* B **63** 201304
[18] Baldassarri H v H G, Bissiri M, Polimeni A, Capizzi M, Fischer M, Reinhardt M and Forchel A 2001 *Appl. Phys. Lett.* **78** 3472
[19] Bissiri M, Baldassarri G, Polimeni A, Capizzi M, Gollub D, Fischer M, Reinhardt M and Forchel A 2002 *Phys. Rev.* B **66** 033311
[20] Bissiri M, Baldassarri H v H G, Polimeni A, Gaspari V, Ranalli F, Capizzi M, Amore Bonapasta A, Jiang F, Stavola M, Gollub D, Fischer M and Forchel A 2002 *Phys. Rev.* B **65** 235210
[21] Amore Bonapasta A, Filippone F, Giannozzi P, Capizzi M and Polimeni A 2002 *Phys. Rev. Lett.* **89** 216401
[22] Klar P J, Grüning H, Heimbrodt W, Koch J, Höhnsdorf F, Stolz W, Vicente P M A and Camassel J 2000 *Appl. Phys. Lett.* **76** 3439
[23] Grüning H, Chen L, Hartmann T, Klar P J, Heimbrodt W, Höhnsdorf F, Koch J and Stolz W 1999 *Phys. Status Solidi* b **215** 39
[24] Makimoto T and Kobayashi N 1995 *Appl. Phys. Lett.* **67** 688
[25] Shima T, Makita Y, Kimura S, Sanpei H, Fukuzawa Y, Sandhu A and Nakamura Y 1999 *Appl. Phys. Lett.* **74** 2675
[26] Makimoto T, Saito H, Nishida T and Kobayashi N 1997 *Appl. Phys. Lett.* **70** 2984
[27] Zhang Y, Mascarenhas A, Geisz J F, Xin H P and Tu C W 2001 *Phys. Rev.* B **63** 085205
[28] Francoeur S, Nikishin S A, Jin C, Qiu Y and Temkin H 1999 *Appl. Phys. Lett.* **75** 1538
[29] Tisch U, Finkman E and Salzman J 2002 *Appl. Phys. Lett.* **81** 463
[30] Rossi J A, Wolfe C M and Dimmock J O 1970 *Phys. Rev. Lett.* **25** 1614
[31] Rühle W and Göbel E 1976 *Phys. Status Solidi* b **78** 311
[32] Dean P J, Venghaus H and Simmonds P E 1978 *Phys. Rev.* B **18** 6813
[33] Zemon S, Norris P, Koteles E S and Lambert G 1986 *J. Appl. Phys.* **59** 2828

[34] Polimeni A, Bissiri M, Felici M, Capizzi M, Buyanova I A, Chen W M, Xin H P and Tu C W 2003 *Phys. Rev.* B **67** 201303
[35] Polimeni A, Ciatto G, Ortega L, Jiang F, Boscherini F, Filippone F, Amore Bonapasta A, Stavola M and Capizzi M 2003 *Phys. Rev.* B **68** 085204
[36] MacDonald A H and Ritchie D S 1986 *Phys. Rev.* B **33** 8336
[37] Wimbauer Th, Oettinger K, Efros Al L, Meyer B K and Brugger H 1994 *Phys. Rev.* B **50** 8889
[38] Bastard G, Mendez E E, Chang L L and Esaki L 1982 *Phys. Rev.* B **26** 1974
[39] Mattila T, Wei Sh-H and Zunger A 1999 *Phys. Rev.* B **60** R11245
[40] Kent P R C and Zunger A 2001 *Phys. Rev.* B **64** 115208
[41] Oueslati M, Benoit a la Guillaume C and Zouaghi M 1988 *Phys. Rev.* B **37** 3037
[42] Cohen E and Sturge M D 1982 *Phys. Rev.* B **25** 3828
[43] Ouadjaout D and Marfaing Y 1990 *Phys. Rev.* B **41** 12096
[44] Kim H S, Mair R A, Li J, Lin J Y and Jiang H X 2000 *Appl. Phys. Lett.* **76** 1252
[45] Ouadjaout D and Marfaing Y 1992 *Phys. Rev.* B **46** 7908
[46] Aït-Ouali A, Chennouf A, Yip Y-F, Brebner J L, Leonelli R and Masut R A 1998 *J. Appl. Phys.* **84** 5639
[47] Buyanova I A, Chen W M, Bergman J P, Monemar B, Xin H P and Tu C W 1999 *Appl. Phys. Lett.* **75** 501
[48] Mair R A, Lin J Y, Jiang H X, Jones E D and Kurtz S R 2000 *Appl. Phys. Lett.* **76** 188
[49] Luo X D, Xu Z Y, Ge W K, Pan Z, Li L H and Lin Y W 2001 *Appl. Phys. Lett.* **79** 958
[50] Kaschner A, Lüttgert T, Born H, Hoffmann A, Egorov A Yu and Riechert H 2001 *Appl. Phys. Lett.* **78** 1391
[51] Vinattieri A, Alderighi D, Zamfirescu M, Colocci M, Polimeni A, Capizzi M, Gollub D, Fischer M and Forchel A 2003 *Appl. Phys. Lett.* **82** 2805
[52] Sun B Q, Gal M, Gao Q, Tan H H and Jagadish C 2002 *Appl. Phys. Lett.* **81** 4368
[53] Hopfield J J, Thomas D G and Lynch R T 1966 *Phys. Rev. Lett.* **17** 312
[54] Vurgaftman I, Meyer J R and Ram-Mohan L R 2001 *J. Appl. Phys.* **89** 5815
[55] MacDonald A H 2002 private communication